Applied Energy 212 (2018) 1578–1588

Contents lists available at ScienceDirect

Applied Energy

journal homepage: www.elsevier.com/locate/apenergy

Teaching–learning–based artificial bee colony for solar photovoltaic parameter estimation

Xu Chen[a,b,*], Bin Xu[c], Congli Mei[a], Yuhan Ding[a], Kangji Li[a]

[a] School of Electrical and Information Engineering, Jiangsu University, Zhenjiang 212013, Jiangsu, China
[b] Key Laboratory of Advanced Control and Optimization for Chemical Processes, Ministry of Education, East China University of Science and Technology, Shanghai 200237, China
[c] School of Mechanical Engineering, Shanghai University of Engineering Science, Shanghai 201620, China

HIGHLIGHTS

- Teaching-learning-based artificial bee colony algorithm is proposed.
- Three hybrid teaching-learning-based bee search phases are presented.
- The method is applied to solve three photovoltaic parameters estimation problems.
- It achieves very competitive results in terms of accuracy and reliability.

ARTICLE INFO

Keywords:
Photovoltaic parameter estimation
Metaheuristic algorithm
Teaching-learning-based optimization
Artificial bee colony
Hybridization

ABSTRACT

Parameters estimation of photovoltaic (PV) model based on experimental data plays an important role in the simulation, evaluation, control, and optimization of PV systems. In the past decade, many metaheuristic algorithms have been used to extract the PV parameters; however, developing hybrid algorithms based on two or more metaheuristic algorithms may further improve the accuracy and reliability of single metaheuristic algorithms. In this paper, by combining teaching-learning-based optimization (TLBO) and artificial bee colony (ABC), we propose a new hybrid teaching-learning-based artificial bee colony (TLABC) for the solar PV parameter estimation problems. The proposed TLABC employs three hybrid search phases, namely teaching-based employed bee phase, learning-based on looker bee phase, and generalized oppositional scout bee phase to efficiently search the optimization parameters. TLABC is applied to identify parameters of different PV models, including single diode, double diode, and PV module, and the results of TLABC are compared with well-established TLBO and ABC algorithms, as well as those results reported in the literature. Experimental results show that TLABC can achieve superior performance in terms of accuracy and reliability for different PV parameter estimation problems.

1. Introduction

Energy crisis, environmental pollution, climate change, and fuel exhaustion are crucial challenges that highlight the importance of using alternative renewable energy sources [1]. Among renewable energy sources such as wind, wave, nuclear, tidal, geothermal, biomass, and so on, solar energy is regarded as one of those with the most potential due to its wide availability and cleanliness [2]. According to [3], the solar PV was the world's leading source of additional power generating capacity in 2016. The annual market increased nearly 50%, equivalent to more than 31,000 solar panels installed every hour. Moreover, PV is an emission-free distributed generation system that is able to directly convert solar energy to electricity and supply power for specific purposes [4]. Solar energy can be converted into electrical energy through photovoltaic (PV) technology [5]. Accurate modeling of PV modules helps in designing and assessing PV systems. The accuracy of PV models mainly depends on their model parameters that usually are unavailable and will change due to aging and faults [6]. Hence, it is indispensable to identify the PV model parameters based on experimental current-voltage data, and this motivates the development of various parameter estimation techniques over recent years [7].

The current estimation techniques for PV parameters can be divided into analytical methods and numerical methods. Analytical methods represent model parameters mathematically by a series of equations on

* Corresponding author at: School of Electrical and Information Engineering, Jiangsu University, Zhenjiang 212013, Jiangsu, China.
E-mail address: xuchen@ujs.edu.cn (X. Chen).

https://doi.org/10.1016/j.apenergy.2017.12.115
Received 3 October 2017; Received in revised form 2 December 2017; Accepted 30 December 2017

the basis of experimental characteristics [8]. This method is easy to implement, however, the accuracy of analytical solution greatly relies on the values of selected points. Inaccurate values may lead to a solution with significant error in some cases. In addition, analytical approaches often need to make some assumptions and/or approximations, which may also cause a loss in solution accuracy [9].

To overcome the disadvantage in the analytical methods, many researchers have explored numerical methods, which include the deterministic and metaheuristic. Deterministic methods such as Newton-Raphson method [10], Lambert W-functions [11], and the iterative curve fitting [12], are generally gradient-based methods. They are tend to be trapped in local optimal. In addition, many deterministic methods are highly sensitive to the initial values, thus leading to a lower efficiency when the initial point is far from the global optimal.

Metaheuristic methods have advantages such as imposing no restrictions on the problem formulation, conceptual and computational simplicity, and being excellent for multimodal problem [13]. Therefore, more recently, many researchers have proposed the use of metaheuristic methods for PV parameter estimation, such as genetic algorithms [14–16], particle swarm optimization [17,18], differential evolution [19–22], simulated annealing [23], harmony search [24], teaching learning based optimization [7,13,25], artificial bee colony [26,27], biogeography-based optimization [28], shuffled frog leaping algorithm [29], cuckoo search [30], and flower pollination algorithm [2,31,32], bacterial foraging algorithm [33], moth-flame optimization [34], whale optimization algorithm [4], cat swarm optimization [9], imperialist competitive algorithm [35], water cycle algorithm [36], ant lion optimizer [37], multi-verse optimizer [38], and Jaya algorithm [39,40].

Hybridization is the process of combining the best features of two or more algorithms in order to create a new algorithm that is expected to outperform its ancestors [41]. Although many metaheuristic algorithms have been used to extract the PV parameters, developing hybrid metaheuristic algorithms based on two or more metaheuristic algorithms may further improve the accuracy and reliability of single metaheuristic algorithms. Therefore, in this study, a new hybrid algorithm called teaching-learning-based artificial bee colony (TLABC) is proposed to effectively and accurately identify the parameters of PV models. The proposed method is based on two metaheuristic algorithms namely teaching-learning-based optimization (TLBO) and artificial bee colony (ABC). TLBO [42] is inspired by the teaching and learning process of a typical class, and it uses two operators namely teacher phase and learner phase to search good solutions. ABC [43] is inspired by the intelligent foraging behavior of honey bees, and it uses three kinds of bees, namely employed bees, onlooker bees, and scout bees, to find good solutions. Previous studies show that TLBO is good at exploitation [44], while ABC has a good exploration for global optimization [45]. As a good search process needs to balance both exploration and exploitation; therefore, this study proposes a hybrid TLABC algorithm, aiming at combining the good exploitation of TLBO and good exploration of ABC.

The main contributions of this study are as follows:

(1) By combining the features of TLBO and ABC, a new hybrid metaheuristic algorithm called teaching-learning-based artificial bee colony (TLABC) is proposed for solar photovoltaic parameter estimation.
(2) TLABC employs three hybrid search phases, i.e., teaching-based employed bee phase, learning-based on looker bee phase, and generalized oppositional scout bee phase to search good solutions.
(3) TLABC is applied to solve three parameters estimation problems of different PV models, and its performance is extensively compared with previous well-established TLBO and ABC algorithms, as well as those results reported in the literature.

The rest of this paper is organized as follows. Section 2 states the problem formulations of photovoltaic models. Section 3 briefly introduces the TLBO and ABC. Section 4 presents the proposed TLABC algorithm in detail. Section 5 displays the experimental results on the PV parameters estimation problems. Finally, Section 6 concludes this paper.

2. Photovoltaic models and problem formulation

This section describes three equivalent circuit models that describe the current-voltage characteristics of the solar cells and photovoltaic modules. They are the single-diode, double-diode and PV module models.

2.1. Single diode model

In the single diode model, as shown in Fig. 1(a), the output current of solar cell can be formulated as follows [16,19]:

$$I_L = I_{ph} - I_d - I_{sh} \tag{1}$$

where I_L is the cell output current, I_{ph} is the photo generated current, I_d is the diode currents, and I_{sh} is the shunt resistor current. According the Shockley equation, the diode currents can be calculated as:

$$I_d = I_{sd}\left(\exp\left(\frac{V_L + I_L R_S}{aV_t}\right) - 1\right) \tag{2}$$

where I_{sd} is reverse saturation current of diode, V_L is the cell output voltage, a is the diode ideality constants, R_S is the series resistance, and V_t is the junction thermal voltage as:

$$V_t = \frac{kT}{q} \tag{3}$$

where k is the Boltzmann constant (1.3806503×10^{23} J/K), T is the temperature of the junction in Kelvin, and q is the electron charge ($1.60217646 \times 10^{-19}$ C).

The shunt resistor current I_{sh} is formulated as

$$I_{sh} = \frac{V_L + I_L R_s}{R_{sh}} \tag{4}$$

where R_{sh} denotes the shunt resistance.

Therefore, by combining Eqs. (1)–(4), the relationship among the output current, output voltage, and model parameters for the single diode model is given by Eq. (5).

$$I_L = I_{ph} - I_{sd}\cdot\left[\exp\left(\frac{V_L + R_S\cdot I_L}{a\cdot V_t}\right) - 1\right] - \frac{V_L + R_S\cdot I_L}{R_{sh}} \tag{5}$$

In the above single diode model, there are five parameters (i.e., I_{ph}, I_{sd}, R_S, R_{sh} and a) that need to be extracted from the I–V data of the solar cell.

2.2. Double diode model

The single diode models inherently neglect the effect of recombination current loss in the depletion region. Consideration of this loss, particularly at low voltage, leads to a more precise solution, known as the two-diode model, with reference to Fig. 1(b). The current-voltage relationship can be formulated as [16,19]:

$$\begin{aligned} I_L &= I_{ph} - I_{d1} - I_{d2} - I_{sh} \\ &= I_{ph} - I_{sd1}\left(\exp\left(\frac{V_L + I_L R_S}{a_1 V_t}\right) - 1\right) - I_{sd2}\left(\exp\left(\frac{V_L + I_L R_S}{a_2 V_t}\right) - 1\right) - \frac{V_L + I_L R_s}{R_{sh}} \end{aligned} \tag{6}$$

where I_{d1} and I_{d2} are the first and second diode currents, I_{sd1} and I_{sd2} are respectively the diffusion and saturation currents, a_1 and a_2 denote the diffusion and recombination diode ideality factors, respectively.

In the double diode model, there are seven parameters (i.e., I_{ph}, I_{sd1}, I_{sd2}, R_s, R_{sh}, a_1 and a_2) that need to be extracted from the I–V data of the solar cell.

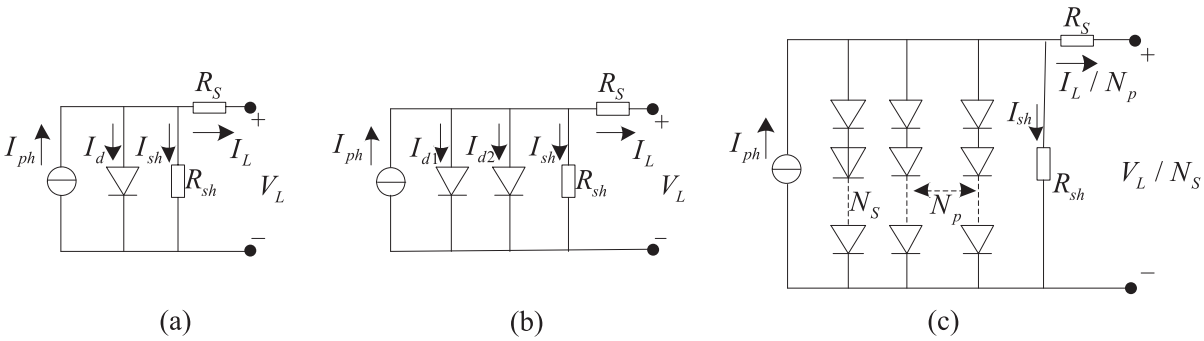

Fig. 1. Equivalent circuit of (a) single-diode, (b) double-diode, and (c) PV module.

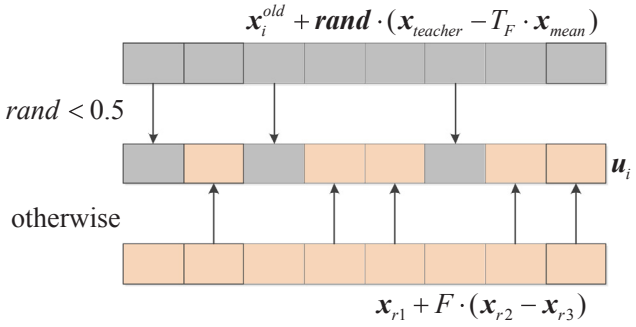

Fig. 2. Hybrid TLBO teaching strategy.

2.3. Single diode PV module model

PV modules usually consists of several solar cells connected in series and/or in parallel [7,33]. Fig. 1(c) gives the schematic of single diode PV module and the current-voltage relationship can be formulated by Eq. (7).

$$I_L/N_p = I_{ph} - I_{sd}\cdot\left[\exp\left(\frac{V_L/N_S + R_S\cdot I_L/N_p}{a\cdot V_t}\right) - 1\right] - \frac{V_L/N_S + R_S\cdot I_L/N_p}{R_{sh}} \tag{7}$$

where N_p and N_s are the number of solar cells in parallel and series, respectively.

2.4. Objective function

In the parameter estimation problem of PV models, the main objective is to minimize the difference between the measured and simulated current data, and the difference usually is quantified by the overall root mean square error (RMSE) [1,13]. Hence, the objective function is formulated as follows:

$$\mathrm{RMSE}(\boldsymbol{x}) = \sqrt{\frac{1}{N}\sum_{k=1}^{N} f(V_L, I_L, \boldsymbol{x})^2} \tag{8}$$

where N is the number of experimental data.

In Eq. (8), for the single diode model,

$$\begin{cases} f_{\mathrm{single}}(V_L, I_L, \boldsymbol{x}) = I_{ph} - I_{sd}\left(\exp\left(\frac{V_L + I_L R_S}{aV_t}\right) - 1\right) - \frac{V_L + I_L R_s}{R_{sh}} - I_L \\ \boldsymbol{x} = \{I_{ph}, I_{sd}, R_S, R_{sh}, a\} \end{cases} \tag{9}$$

For the double diode model,

$$\begin{cases} f_{\mathrm{double}}(V_L, I_L, \boldsymbol{x}) = I_{ph} - I_{sd1}\left(\exp\left(\frac{V_L + I_L R_S}{a_1 V_t}\right) - 1\right) - I_{sd2}\left(\exp\left(\frac{V_L + I_L R_S}{a_2 V_t}\right) - 1\right) \\ \qquad\qquad - \frac{V_L + I_L R_s}{R_{sh}} - I_L \\ \boldsymbol{x} = \{I_{ph}, I_{sd1}, I_{sd2}, R_S, R_{sh}, a_1, a_2\} \end{cases} \tag{10}$$

For the single diode PV module model,

$$\begin{cases} f_{\mathrm{module}}(V_L, I_L, \boldsymbol{x}) = N_p I_{ph} - N_p I_{sd}\left[\exp\left(\frac{V_L/N_S + R_S I_L/N_p}{aV_t}\right) - 1\right] - \frac{N_p V_L/N_S + R_S I_L}{R_{sh}} \\ \qquad\qquad - I_L \\ \boldsymbol{x} = \{I_{ph}, I_{sd}, R_S, R_{sh}, a\} \end{cases} \tag{11}$$

The values of I_L and V_L are experimentally collected from current-voltage measurements of the PV models. Thus, the parameter estimation is a process that minimizes the objective function RMSE ($\boldsymbol{x}$) by adjusting the model parameters vector $\boldsymbol{x}$ within the range of a given bound.

3. Introductions to TLBO and ABC

3.1. Teaching-learning-based optimization

TLBO is a population-based optimization method which mimics the teaching and learning process of a typical class [42]. In TLBO, The class $\{\boldsymbol{x}_1, \boldsymbol{x}_2, \ldots, \boldsymbol{x}_{NP}\}$ is composed of one teacher and some learners, where $\boldsymbol{x}_i = (x_{i1}, \ldots, x_{ij}, \ldots, x_{iD})$ $(i = 1,2,\ldots,NP)$ denotes the i-th learner, NP is the class size, D represents the number of major subjects in the class; x_{ij} represents the learning status of j-th learner on i-th major subject. The optimization process of TLBO is divided into two stages: teacher phase and learner phase.

In the teacher phase, the teacher provides knowledge to the learners to increase the mean result of the class. The learner with the best fitness in the current generation is identified as the teacher $\boldsymbol{x}_{teacher}$, and the mean position is represented as $\boldsymbol{x}_{mean} = \frac{1}{NP}\sum_{i=1}^{NP}\boldsymbol{x}_i$. The position of each learner is updated by Eq. (12):

$$\boldsymbol{x}_i^{new} = \boldsymbol{x}_i^{old} + \boldsymbol{rand}\cdot(\boldsymbol{x}_{teacher} - T_F\cdot\boldsymbol{x}_{mean}) \tag{12}$$

where $\boldsymbol{x}_i^{new}$ and $\boldsymbol{x}_i^{old}$ are the i-th learner's new and old positions, respectively, $\boldsymbol{rand}$ is a random vector uniformly distributed within $[0,1]^D$, $T_F = round[1 + rand(0,1)]$ is the teacher factor, and its value is heuristically set to either 1 or 2. If $\boldsymbol{x}_i^{new}$ is better than $\boldsymbol{x}_i^{old}$, $\boldsymbol{x}_i^{new}$ is accepted and flowed to the learner phase, otherwise $\boldsymbol{x}_i^{old}$ is unchanged.

In the learner phase, each learner randomly interacts with other different learners to further improve his/her performance. Learner $\boldsymbol{x}_i$ randomly selects another learner $\boldsymbol{x}_j$ $(j \neq i)$ and the learning process can be expressed by Eq. (13):

$$\boldsymbol{x}_i^{new} = \begin{cases} \boldsymbol{x}_i^{old} + \boldsymbol{rand}\cdot(\boldsymbol{x}_i - \boldsymbol{x}_j), & \text{if } f(\boldsymbol{x}_i) \leqslant f(\boldsymbol{x}_j) \\ \boldsymbol{x}_i^{old} + \boldsymbol{rand}\cdot(\boldsymbol{x}_j - \boldsymbol{x}_i), & \text{if } f(\boldsymbol{x}_j) > f(\boldsymbol{x}_i) \end{cases} \tag{13}$$

If $\boldsymbol{x}_i^{new}$ is better than $\boldsymbol{x}_i^{old}$, $\boldsymbol{x}_i^{new}$ is used to replace $\boldsymbol{x}_i^{old}$, otherwise $\boldsymbol{x}_i^{old}$ is unchanged.

3.2. Artificial bee colony

ABC is a swarm intelligence algorithm based on the foraging behavior of honey bee swarms [43]. In ABC, a food source position

Algorithm 1. Teaching-learning-based artificial bee colony

Stage 1: Initialization

For each index $i = 1,2,\cdots,NP$

Initialize the position of individual $\boldsymbol{x}_i$;

Calculate the objective function value $f(\boldsymbol{x}_i)$ using Eq. (8) and the fitness $fit(\boldsymbol{x}_i)$ using Eq. (15);

Set $trial(i) = 0$ for each individual;

End For

Stage 2: Teaching-based employed bee phase

For each index $i = 1,2,\cdots,NP$

Generate a new candidate solution $\boldsymbol{u}_i$ by hybrid TLBO teaching strategy using Eq.(18);

Calculate the objective function value $f(\boldsymbol{u}_i)$ using Eq. (8) and the fitness value $fit(\boldsymbol{u}_i)$ using Eq. (15);

Apply a greedy selection process between $\boldsymbol{u}_i$ and $\boldsymbol{x}_i$ to select the better one;

If solution $\boldsymbol{x}_i$ does not improve, $trial(i) = trial(i) + 1$, otherwise $trial(i) = 0$;

End For

Stage 3: Learning-based on looker bee phase

Calculate the selection probability p_i using Eq.(17);

For each index $i = 1,2,\cdots,NP$

Select a solution $\boldsymbol{x}_s$ using the roulette method according to the probability p_i ;

Generate a new candidate solution $\boldsymbol{u}_s$ by TLBO learning strategy using Eq.(19) ;

Calculate the objective function value $f(\boldsymbol{u}_s)$ using Eq. (8) and the fitness value $fit(\boldsymbol{u}_s)$ using Eq. (15);

Apply a greedy selection process between $\boldsymbol{u}_s$ and $\boldsymbol{x}_s$ to select the better one.

If solution $\boldsymbol{x}_s$ does not improve, $trial(s) = trial(s) + 1$, otherwise $trial(s) = 0$.

End For

Stage 4: Generalized oppositional scout bee phase

If $\max(trial(i)) \geq \text{limit}$, **Then**

Generate a new random candidate solution $\boldsymbol{x}_i$ and its generalized oppositional solution $\boldsymbol{x}_i^{GO}$;

Replace the old $\boldsymbol{x}_i$ with the better one between the new $\boldsymbol{x}_i$ and $\boldsymbol{x}_i^{GO}$;

End If

Stage 5: If the stop criterion is satisfied, stop and output the best solution achieved so far. Otherwise, return to Step 2.

Fig. 3. Framework of TLABC.

Table 1
Parameters range of the single and double diode models, and PV module model.

Parameter	Single and double diode		PV module	
	Lower bound	Upper bound	Lower bound	Upper bound
I_{ph} (A)	0	1	0	2
I_{sd} (μA)	0	1	0	50
R_S (Ω)	0	0.5	0	2
R_{sh} (Ω)	0	100	0	2000
a	1	2	1	50

represents a potential solution to the optimization problem. It implements a cycle of the employed bee phase, onlooker bee phase and scout bee phase until the termination condition is satisfied.

First, the ABC algorithm starts with randomly producing NP food sources:

$$x_{ij} = x_{\min,j} + (x_{\max,j} - x_{\min,j}) \cdot rand_1 \quad (14)$$

Table 2
Parameter settings for TLABC and the compared ABC and TLBO algorithms.

Algorithm	Parameter settings
TLBO	Population size $NP = 50$
NIWTLBO	$NP = 50$, inertia weight $w = 0 \sim 1.0$
LETLBO	$NP = 50$
GOTLBO	$NP = 50$, jumping rate $Jr = 0.3$
ABC	$NP = 50$, $limit = 200$
GABC	$NP = 50$, $limit = 200$, $C = 1.5$
MABC	$NP = 50$, $limit = 200$, modification rate $MR = 0.4$, scaling factor $SF = 1$
GBABC	$NP = 50$, $limit = 200$, crossover rate $CR = 0.3$
TLABC	$NP = 50$, $limit = 200$, scale factor $F = rand(0,1)$

where $\boldsymbol{x}_i = (x_{i1}, x_{i2}, \ldots, x_{iD})$, $i \in \{1,2,\ldots,NP\}$ represents the i-th solution; $\boldsymbol{x}_{\min,j}$ and $\boldsymbol{x}_{\max,j}$ are the lower and upper bounds for the dimension j, respectively; $rand_1$ is a random number within [0, 1]. The fitness values of the food sources are then calculated as:

Table 3
Comparison among TLABC and the ABC and TLBO algorithms for the single diode model.

Item	I_{ph} (A)	I_{sd} (μA)	R_s (Ω)	R_{sh} (Ω)	a	RMSE	Rank
TLBO	0.76074	0.32938	0.0363	54.3015	1.48314	9.87332E−04	5
NIWTLBO	0.76078	0.32314	0.03638	53.69219	1.48122	9.86025E−04	2
LETLBO	0.76078	0.32223	0.03639	53.66548	1.48094	9.86034E−04	3
GOTLBO	0.76077	0.32256	0.03637	53.33877	1.48106	9.86578E−04	4
ABC	0.76085	0.33016	0.03629	53.59884	1.48339	9.88148E−04	8
GABC	0.76091	0.33541	0.03609	50.03902	1.48518	9.96438E−04	9
MABC	0.76079	0.32247	0.03639	53.80993	1.48099	9.88080E−04	7
GBABC	0.76073	0.3328	0.03625	54.63205	1.4842	9.88006E−04	6
TLABC	0.76078	0.32302	0.03638	53.71636	1.48118	9.86022E−04	1

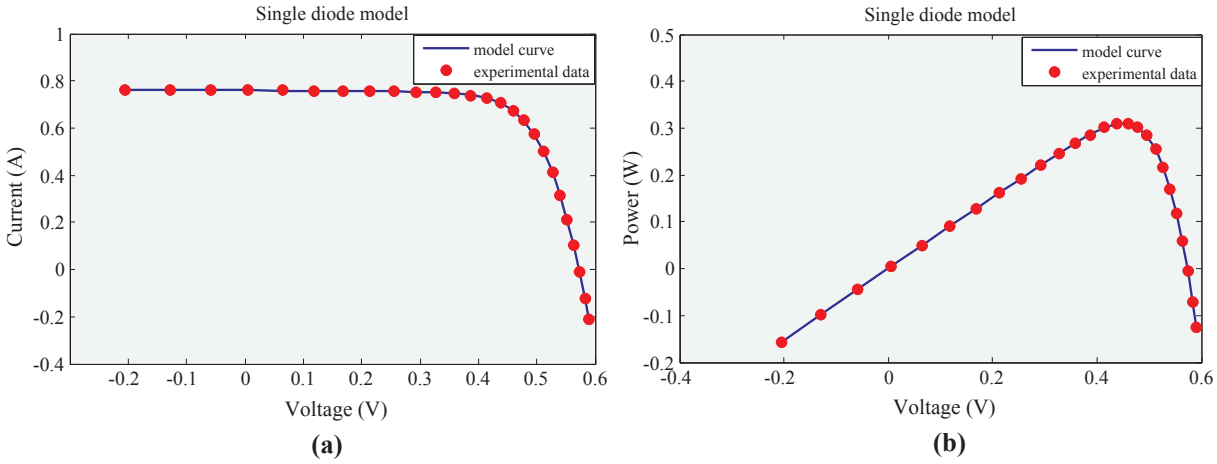

Fig. 4. Comparisons between experimental data and simulated data obtained by TLABC for single diode model (a) *I-V* characteristics and (b) *P-V* characteristics.

Table 4
The calculated current and absolute error results of TLABC for the single diode model.

Item	V_L (V)	I_L (A)	I_L calculated (A)	IAE
1	−0.2057	0.7640	0.76408804	0.00008804
2	−0.1291	0.7620	0.76266337	0.00066337
3	−0.0588	0.7605	0.76135554	0.00085554
4	0.0057	0.7605	0.76015417	0.00034583
5	0.0646	0.7600	0.75905535	0.00094465
6	0.1185	0.7590	0.75804244	0.00095756
7	0.1678	0.7570	0.75709172	0.00009172
8	0.2132	0.7570	0.75614139	0.00085861
9	0.2545	0.7555	0.75508687	0.00041313
10	0.2924	0.7540	0.75366385	0.00033615
11	0.3269	0.7505	0.75139092	0.00089092
12	0.3585	0.7465	0.74735378	0.00085378
13	0.3873	0.7385	0.74011715	0.00161715
14	0.4137	0.7280	0.72738215	0.00061785
15	0.4373	0.7065	0.70697259	0.00047259
16	0.4590	0.6755	0.67528012	0.00021988
17	0.4784	0.6320	0.63075828	0.00124172
18	0.4960	0.5730	0.57192842	0.00107158
19	0.5119	0.4990	0.49960712	0.00060712
20	0.5265	0.4130	0.41364892	0.00064892
21	0.5398	0.3165	0.31751024	0.00101024
22	0.5521	0.2120	0.21215504	0.00015504
23	0.5633	0.1035	0.10225134	0.00124866
24	0.5736	−0.0100	−0.00871762	0.00128238
25	0.5833	−0.1230	−0.12550764	0.00250764
26	0.5900	−0.2100	−0.20847269	0.00152731
Sum of IAE				0.02152738

$$fit(\boldsymbol{x}_i) = \begin{cases} \frac{1}{1+f(\boldsymbol{x}_i)} & if\ f(\boldsymbol{x}_i) \geqslant 0 \\ 1 + |f(\boldsymbol{x}_i)| & otherwise \end{cases} \tag{15}$$

where $f(\boldsymbol{x}_i)$ is the objective function value of $\boldsymbol{x}_i$.

In the employed bee phase, each employed bee performs a modification on the position of the food source by randomly selecting a neighboring food source. A new food source $\boldsymbol{u}_i = (u_{i1},u_{i2},...,u_{iD})$ can be generated from the old food source as follows:

$$u_{ij} = x_{ij} + \psi\cdot(x_{ij}-x_{kj}) \tag{16}$$

where $k \in \{1,2,...,NP\}$ is a randomly chosen index and must be different from i; ψ is a random number in the range $[-1, 1]$.

In the onlooker bee phase, an onlooker bee selects a food source to seek out according to the selection probability p, which is calculated as

$$p_i = \frac{fit(\boldsymbol{x}_i)}{\sum_{i=1}^{SN} fit(\boldsymbol{x}_i)} \tag{17}$$

where *fit* is the fitness value of the solution, which is calculated using Eq. (15).

After the onlooker bee selects a food source $\boldsymbol{x}_s$ to seek out, a candidate food source position $\boldsymbol{u}_s = (u_{s1},u_{s2},...,u_{sD})$ will be produced by using Eq. (16).

If the food source position of the employed bees cannot be further improved through a given number of steps (*limit*) in the ABC algorithm, this employed bee becomes a scout bee. The new random food source position (scout bee) will be generated from the Eq. (14).

The candidate solution is compared with the old one. If the new food source has a better quality than the old source, then the old source is replaced by the new one. Otherwise, the old source is retained.

Table 5
Comparison among TLABC and the other algorithms for the double diode model.

Item	I_{ph} (A)	I_{sd1} (μA)	R_s (Ω)	R_{sh} (Ω)	a_1	I_{sd2} (μA)	a_2	RMSE	Rank
TLBO	0.76099	0.29465	0.03661	53.12099	1.47295	0.13727	1.99375	1.00692E−03	9
NIWTLBO	0.7608	0.2843	0.03651	53.70554	1.47026	0.27081	1.9996	9.84618E−04	2
LETLBO	0.76081	0.11366	0.03642	54.06878	1.92836	0.30317	1.47597	9.85712E−04	4
GOTLBO	0.76081	0.27173	0.03655	53.61867	1.46681	0.25952	1.91606	9.85437E−04	3
ABC	0.76071	0.14623	0.03654	55.36509	1.68023	0.24605	1.46226	9.89560E−04	6
GABC	0.76089	0.32391	0.03638	52.98993	1.48146	7.00E−05	1.99282	9.88625E−04	5
MABC	0.76071	0.2175	0.03651	55.22908	1.45606	0.16555	1.63102	9.92030E−04	8
GBABC	0.76073	0.57372	0.0369	55.9381	1.92862	0.21689	1.44779	9.90699E−04	7
TLABC	0.76081	0.42394	0.03667	54.66797	1.9075	0.24011	1.45671	9.84145E−04	1

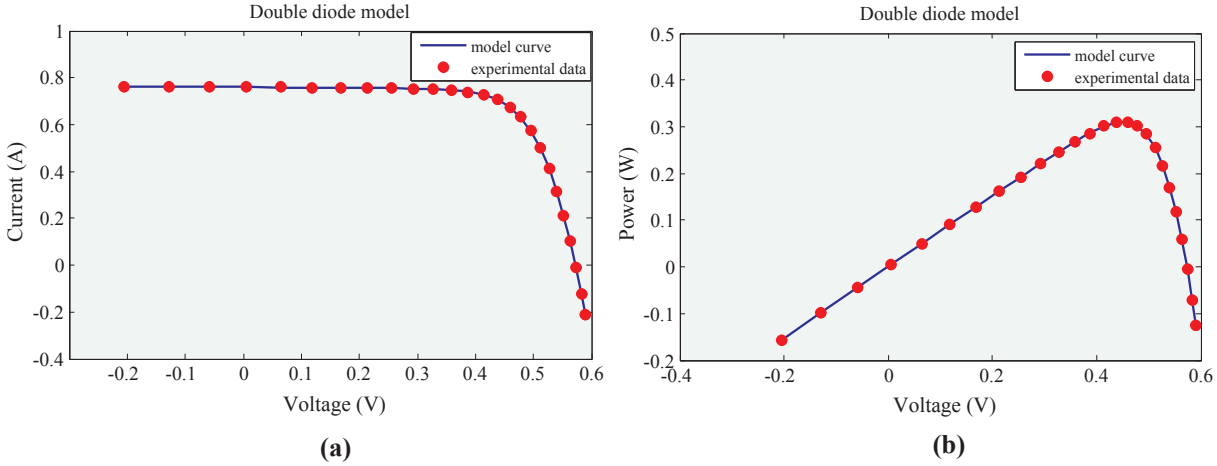

Fig. 5. Comparisons between experimental data and simulated data obtained by TLABC for double diode model (a) I-V characteristics and (b) P-V characteristics.

Table 6
The calculated current and absolute error results of TLABC for the double diode model.

Item	V_L (V)	I_L (A)	I_L calculated (A)	IAE
1	−0.2057	0.7640	0.76406184	0.00002620
2	−0.1291	0.7620	0.76266194	0.00000143
3	−0.0588	0.7605	0.76137673	0.00002119
4	0.0057	0.7605	0.76019582	0.00004165
5	0.0646	0.7600	0.75911482	0.00005947
6	0.1185	0.7590	0.75811628	0.00007384
7	0.1678	0.7570	0.75717481	0.00008309
8	0.2132	0.7570	0.75622613	0.00008474
9	0.2545	0.7555	0.75516281	0.00007594
10	0.2924	0.7540	0.75371858	0.00005473
11	0.3269	0.7505	0.75141326	0.00002234
12	0.3585	0.7465	0.74733795	0.00001583
13	0.3873	0.7385	0.74006828	0.00004887
14	0.4137	0.7280	0.72731735	0.00006480
15	0.4373	0.7065	0.70691842	0.00005417
16	0.4590	0.6755	0.67525961	0.00002051
17	0.4784	0.6320	0.63077856	0.00002028
18	0.4960	0.5730	0.57197740	0.00004898
19	0.5119	0.4990	0.49965911	0.00005199
20	0.5265	0.4130	0.41366985	0.00002093
21	0.5398	0.3165	0.31748038	0.00002986
22	0.5521	0.2120	0.21206942	0.00008562
23	0.5633	0.1035	0.10213126	0.00012008
24	0.5736	−0.0100	−0.00880471	0.00008709
25	0.5833	−0.1230	−0.12553039	0.00002275
26	0.5900	−0.2100	−0.20835510	0.00011759
Sum of IAE				0.00135397

4. Teaching-learning-based artificial bee colony

TLBO employs two production operators namely teaching and learning to search solutions. It is good at exploitation, but its exploration is relative poor for complex problems [44]. On the other hand, ABC uses three search phases, namely employed bee phase, onlooker bee phase, and scout bee phase, to explore solutions. ABC has a good exploration for global optimization but poor at exploitation [45]. In order to balance the exploration and the exploitation during the searching process, this section proposes a hybrid teaching–learning artificial bee colony (TLABC) algorithm, which combines the exploitation of TLBO with the exploration of ABC effectively.

TLABC uses three hybrid search phases to search solutions: (1) teaching-based employed bee phase, (2) learning-based on looker bee phase, and (3) generalized oppositional scout bee phase. These three phases are described in detail below.

4.1. Teaching-based employed bee phase

TLABC starts with initializing NP food sources $\boldsymbol{x}_i = (x_{i1},...,x_{ij},...,x_{iD})$ $(i = 1,2,...,NP)$ using Eq. (14), and calculating the fitness values using Eq. (15).

Then, it enters into the teaching-based employed bee phase, in which each employed bee searches a new food source $\boldsymbol{u}_i = (u_{i1},u_{i2},...,u_{iD})$ using a hybrid TLBO teaching strategy:

$$u_{i,d} = \begin{cases} x_{i,d}^{old} + rand_2 \cdot (x_{teacher,d} - T_F \cdot x_{mean,d}) & if\ rand_1 < 0.5 \\ x_{r1,d} + F \cdot (x_{r2,d} - x_{r3,d}) & else \end{cases} \quad (18)$$

where r_1, r_2, and $r_3 (r_1 \neq r_2 \neq r_3 \neq i)$ are integers randomly selected from $\{1,2,...,NP\}$, $d \in \{1,2,...,D\}$, $rand_1$ and $rand_2$ are two random numbers uniformly distributed within [0,1], and F is a scale factor in [0,1]. If $\boldsymbol{u}_i$ is better than $\boldsymbol{x}_i$, then $\boldsymbol{u}_i$ is used to replace $\boldsymbol{x}_i$.

The hybrid TLBO teaching strategy is shown in Fig. 2. In the basic teaching strategy (i.e., Eq. (12)), all learners use the same differential vector $(\boldsymbol{x}_{teacher} - T_F \cdot \boldsymbol{x}_{mean})$ to update the positions, so the diversity of the search directions is poor. By contrast, the hybrid teaching strategy (i.e.,

Table 7
Comparison among TLABC and the other algorithms for the PV module model.

Item	I_{ph} (A)	I_{sd} (μA)	R_s (Ω)	R_{sh} (Ω)	a	RMSE	Rank
TLBO	1.03049	3.48718	1.20111	984.87604	48.64819	2.42509E−03	3
NIWTLBO	1.0305	3.4834	1.20131	984.23695	48.64399	2.42508E−03	2
LETLBO	1.03051	3.47088	1.20166	981.0293	48.63022	2.42510E−03	4
GOTLBO	1.03046	3.49907	1.2008	989.68885	48.66113	2.42513E−03	5
ABC	1.03008	3.3019	1.20631	968.65121	48.44085	2.44692E−03	9
GABC	1.03047	3.46592	1.20279	1002.48643	48.62308	2.42831E−03	8
MABC	1.03048	3.50818	1.20049	988.99543	48.67129	2.42517E−03	6
GBABC	1.0306	3.50973	1.20049	982.78561	48.67267	2.42592E−03	7
TLABC	1.03056	3.4715	1.20165	972.93567	48.63131	2.42507E−03	1

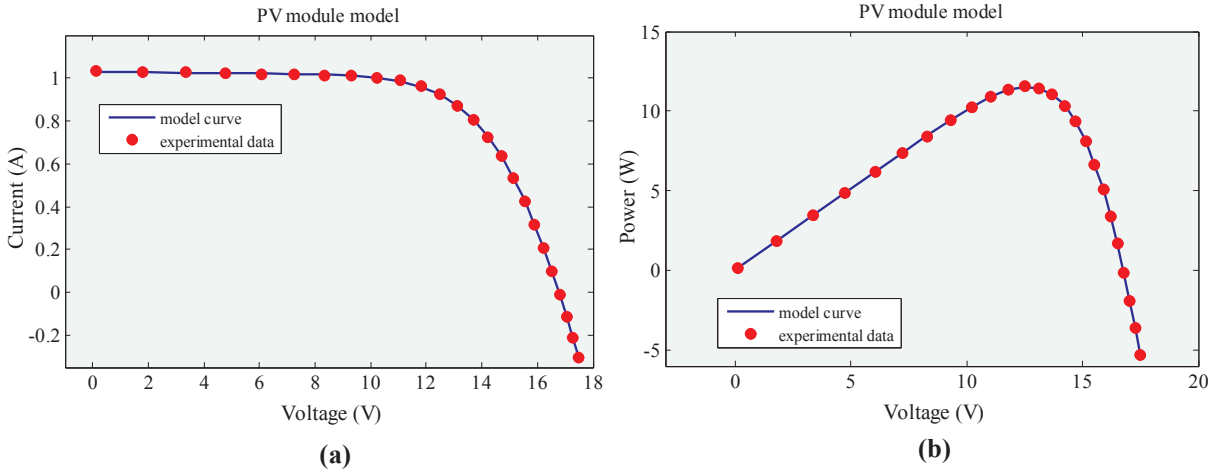

Fig. 6. Comparisons between experimental data and simulated data obtained by TLABC for PV module model (a) I-V characteristics and (b) P-V characteristics.

Table 8
The calculated current and absolute error results of TLABC for the PV module model.

Item	V_L (V)	I_L (A)	I_L calculated (A)	IAE
1	0.1248	1.0315	1.02915327	0.00234673
2	1.8093	1.0300	1.02739930	0.00260070
3	3.3511	1.0260	1.02574561	0.00025439
4	4.7622	1.0220	1.02409798	0.00209798
5	6.0538	1.0180	1.02227114	0.00427114
6	7.2364	1.0155	1.01990019	0.00440019
7	8.3189	1.0140	1.01632474	0.00232474
8	9.3097	1.0100	1.01045224	0.00045224
9	10.2163	1.0035	1.00058206	0.00291794
10	11.0449	0.9880	0.98450102	0.00349898
11	11.8018	0.9630	0.95947594	0.00352406
12	12.4929	0.9255	0.92279589	0.00270411
13	13.1231	0.8725	0.87255969	0.00005969
14	13.6983	0.8075	0.80723639	0.00026361
15	14.2221	0.7265	0.72829984	0.00179984
16	14.6995	0.6345	0.63710199	0.00260199
17	15.1346	0.5345	0.53617787	0.00167787
18	15.5311	0.4275	0.42947861	0.00197861
19	15.8929	0.3185	0.31874639	0.00024639
20	16.2229	0.2085	0.20736920	0.00113080
21	16.5241	0.1010	0.09615760	0.00484240
22	16.7987	−0.0080	−0.00831905	0.00031905
23	17.0499	−0.1110	−0.11091182	0.00008818
24	17.2793	−0.2090	−0.20920162	0.00020162
25	17.4885	−0.3030	−0.30079403	0.00220597
Sum of IAE				0.04880919

Eq. (18)) uses a hybrid of original teaching strategy of TLBO and mutation operator of differential evolution [46], which can improves the diversity of search directions greatly, and it will be very beneficial for the global exploration of teaching-based employed bee phase.

4.2. Learning-based on looker bee phase

After the teaching-based employed bee phase, TLABC enters into the learning-based on looker bee phase. In the learning-based onlooker bee phase, an onlooker bee selects a food source $\boldsymbol{x}_s$ to seek out according to the selection probability p, which is calculated using Eq. (17).

Then, the onlooker bee searches new food sources using the TLBO learning strategy:

$$\boldsymbol{u}_s = \begin{cases} \boldsymbol{x}_s + \boldsymbol{rand}\cdot(\boldsymbol{x}_s - \boldsymbol{x}_j), & \text{if } f(\boldsymbol{x}_s) \leqslant f(\boldsymbol{x}_j) \\ \boldsymbol{x}_s + \boldsymbol{rand}\cdot(\boldsymbol{x}_j - \boldsymbol{x}_s), & \text{if } f(\boldsymbol{x}_j) > f(\boldsymbol{x}_s) \end{cases} \tag{19}$$

where $j \in \{1,2,...,NP\}$ and $j \neq s$. If $\boldsymbol{u}_s$ is better than $\boldsymbol{x}_s$, then $\boldsymbol{u}_s$ is used to replace $\boldsymbol{x}_s$.

4.3. Generalized oppositional scout bee phase

TLABC enters into the generalized oppositional scout bee phase after the learning-based on looker bee phase. The generalized oppositional scout bee phase is proposed in [47], and it uses generalized opposition-based learning strategy [48] to enhance the basic scout bee phase. In this phase, if a food source $\boldsymbol{x}_i$ cannot be improved further for at least *limit* times, it is considered to be exhausted and would be abandoned. Then, a new random candidate solution $\boldsymbol{x}_i = (x_{i1},...,x_{ij},...,x_{iD})$ and its generalized oppositional solution $\boldsymbol{x}_i^{GO} = (x_{i1}^{GO},x_{i2}^{GO},...,x_{iD}^{GO})$ are generated using Eqs. (14) and (20) respectively,

$$x_{ij}^{GO} = k\cdot(a_j + b_j) - x_{ij} \tag{20}$$

where k is a random number in [0,1], and $a_j = \max_i(x_{ij})$, $b_j = \min_i(x_{ij})$.

Then, the better solution between the two solutions $\boldsymbol{x}_i$ and $\boldsymbol{x}_i^{GO}$ are used to replace the old exhausted food source:

Table 9
Statistical results of RMSE of different algorithms for three models.

Model	Algorithm	RMSE			
		Min	Mean	Max	SD
Single diode model	TLBO	9.87332E-04	1.04761E-03	1.23579E-03	6.58940E-05
	NIWTLBO	**9.86025E-04**	**9.89765E-04**	**1.03613E-03**	**9.53115E-06**
	LETLBO	9.86034E-04	1.01274E-03	1.12035E-03	3.13277E-05
	GOTLBO	9.86578E-04	1.07745E-03	1.35363E-03	9.58247E-05
	ABC	9.88148E-04	1.12125E-03	1.41740E-03	1.19818E-04
	GABC	9.96438E-04	1.14685E-03	1.59743E-03	1.44854E-04
	MABC	9.88080E-04	1.09033E-03	1.28838E-03	8.94030E-05
	GBABC	9.88006E-04	1.04412E-03	1.28479E-03	7.40971E-05
	TLABC	**9.86022E-04**	**9.98523E-04**	**1.03970E-03**	**1.86022E-05**
Double diode model	TLBO	1.00692E-03	1.15977E-03	1.52057E-03	1.55921E-04
	NIWTLBO	**9.84618E-04**	**1.00872E-03**	1.35626E-03	**6.86713E-05**
	LETLBO	9.85712E-04	1.08347E-03	1.57168E-03	1.26732E-04
	GOTLBO	9.85437E-04	1.16635E-03	1.59621E-03	1.56170E-04
	ABC	9.89560E-04	1.05765E-03	**1.28482E-03**	**6.18669E-05**
	GABC	9.88625E-04	1.07070E-03	1.45206E-03	9.33815E-05
	MABC	9.92030E-04	1.11974E-03	1.36771E-03	1.09759E-04
	GBABC	9.90699E-04	**1.05267E-03**	**1.27251E-03**	7.00882E-05
	TLABC	**9.84145E-04**	1.05553E-03	1.50482E-03	1.55034E-04
PV module model	TLBO	2.42509E-03	2.43827E-03	2.54750E-03	2.43361E-05
	NIWTLBO	**2.42508E-03**	2.49036E-03	3.99707E-03	2.87409E-04
	LETLBO	2.42510E-03	2.43113E-03	2.46920E-03	9.08036E-06
	GOTLBO	2.42513E-03	2.44733E-03	2.55767E-03	3.14372E-05
	ABC	2.44692E-03	2.50414E-03	2.58639E-03	3.85744E-05
	GABC	2.42831E-03	2.49434E-03	2.56753E-03	3.42016E-05
	MABC	2.42517E-03	**2.42956E-03**	**2.45180E-03**	**6.11861E-06**
	GBABC	2.42592E-03	2.45531E-03	2.53297E-03	2.65586E-05
	TLABC	**2.42507E-03**	**2.42647E-03**	**2.44584E-03**	**3.99568E-06**

The best results are highlighted with shade, and the second best results are highlighted with bold.

$$\boldsymbol{x}_i = \begin{cases} \boldsymbol{x}_i, & \text{if } f(\boldsymbol{x}_i) \leqslant f(\boldsymbol{x}_i^{GO}) \\ \boldsymbol{x}_i^{GO}, & \text{if } f(\boldsymbol{x}_i) > f(\boldsymbol{x}_i^{GO}) \end{cases} \tag{21}$$

4.4. Framework TLABC

Based on the three search phases described above, the framework of TLABC can be summarized in Fig. 3.

5. Results and discussions

In this section, to verify its performance, the proposed TLABC is applied to solve three parameters estimation problems taken from literature. These problems include two cases of solar cells respectively corresponding to the single diode model and the double diode model and a case of the PV module. The experimental *I–V* dataset of the two cases of the solar cell are measured from a 57 mm diameter commercial RTC France silicon solar cell at an irradiance of (1000 W/m^2) and a temperature of (33 °C) and totally contains 26 pairs of current and voltage values. The experimental I–V dataset for the case of the PV module are measured from a Photo watt-PWP 201 PV module in which 36 polycrystalline silicon cells are connected in series at an irradiance of (1000 W/m^2) and a temperature of (45 °C), and totally contains 25 pairs of current and voltage value. The experimental current-voltage data have been widely used by researchers to test the methods developed for parameter estimation [4,6,19,23,24,26,49]. For fair comparison, the lower and upper bounds for each parameter are presented in Table 1, which are the same as used in [4,6,19,23,24,26,49].

To show the effectiveness of the proposed hybrid algorithm, TLABC is compared with eight well-established ABC and TLBO algorithms, they are basic TLBO [42], nonlinear inertia weighted TLBO (NIWTLBO) [50], TLBO with learning experience of other learners (LETLBO) [51], generalized oppositional TLBO (GOTLBO) [13], basic ABC [43], gbest-guided ABC (GABC) [45], modified ABC (MABC) [52], and Gaussian bare-bones ABC (GBABC) [47]. For fair comparison, all the compared algorithms use the same maximum number of function evaluations *MaxFES* = 50,000 [7,25] in each run for each problem. Besides, each algorithm is run 30 times independently to minimize statistical errors. The parameter settings for all the compared algorithms are presented in Table 2.

5.1. Results on single diode model

For the single diode model, the comparison results involving the estimated parameters and RMSE are presented in Table 3. It can be seen that TLABC provides the least RMSE (9.86022E−04) among all the algorithms, followed by NIWTLBO, LETLBO, GOTLBO, TLBO, GBABC, MABC, ABC, and GABC. There are no known accurate parameter values to compare; therefore the RMSE can be used as the index to represent the accuracy.

To further confirm the quality of the results, the best estimated parameters of TLABC are used to reconstruct the *I-V* and *P-V* curves as

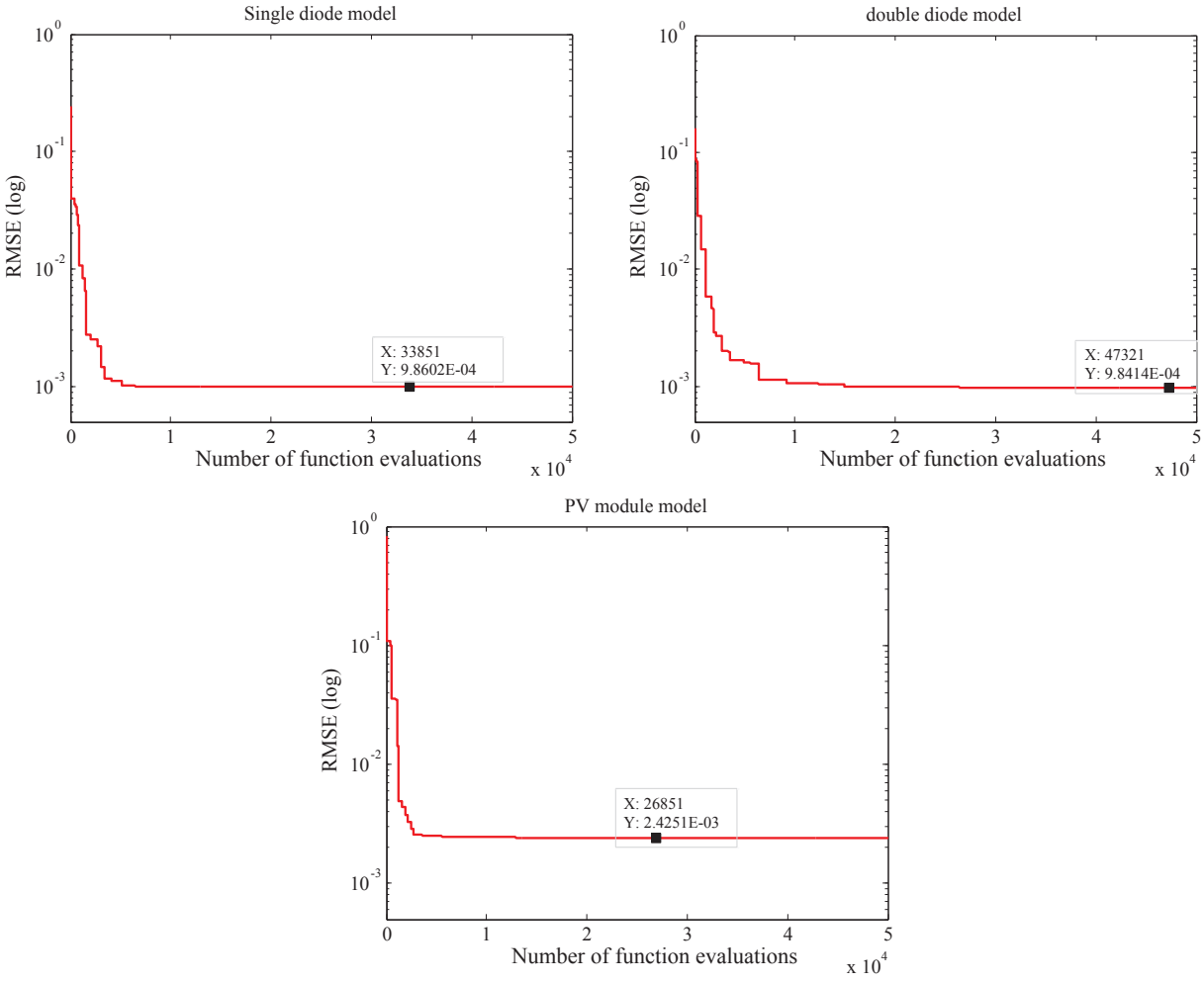

Fig. 7. Convergence curve of TLABC for different PV models.

Table 10
Comparison of TLABC with parameter estimation methods in literature for single diode model.

Item	I_{ph} (A)	I_{sd} (μA)	R_s (Ω)	R_{sh} (Ω)	a	RMSE
GA	0.7619	0.8087	0.0299	42.3729	1.5751	1.9080E−02
CPSO	0.7607	0.4	0.0354	59.012	1.5033	1.3900E−03
PS	0.7617	0.998	0.0313	64.1026	1.6	1.4940E−02
SA	0.762	0.4798	0.0345	43.1034	1.5172	1.9000E−02
IGHS	0.7608	0.3435	0.0361	53.2845	1.4874	9.9306E−04
ABSO	0.7608	0.30623	0.03659	52.2903	1.47878	9.9124E−04
Rcr-IJADE	0.760776	0.323021	0.036377	53.718526	1.481184	9.8602E−04
IJAYA	0.7608	0.3228	0.0364	53.7595	1.4811	9.8603E−04
GOFPANM	0.767755	0.3230208	0.0363771	53.7185203	1.4811836	9.8602E−04
EHA-NMS	0.760776	0.323021	0.036377	53.718521	1.481184	9.8602E−04
CWOA	0.76077	0.3239	0.03636	53.7987	1.4812	9.8602E−04
TLABC	0.76078	0.32302	0.03638	53.71636	1.48118	9.8602E−04

shown in Fig. 4. It is obvious that the calculated data obtained by TLABC are highly in coincidence with the measured data over the whole voltage range. Besides, the individual absolute error (IAE) between the experimental data and simulated data are presented in Table 4. All the IAE values are smaller than 2.508E−03, which proves that the estimated parameters by TLABC are very accurate.

5.2. Results on double diode model

For the double diode model, there are seven parameters need to be identified, and the estimated parameters and the RMSE of different algorithms are listed in Table 5. It is clear that TLABC also provides the best RMSE (9.84145E−04) among all compared algorithms, and NIWTLBO obtains the second best RMSE value. The *I-V* and *P-V* characteristics of the best model parameters estimated by TLABC and the experimental data are given in Fig. 5, and the IAE values are shown in Table 6. From Fig. 5, it can be clearly seen that the calculated data of TLABC are in good agreement with the measured data. From Table 6, all the IAE values are smaller than 1.201E−04, indicating that the high-accurately estimated parameters are provided.

5.3. Results on PV module model

For the PV module model, five parameters need to be identified. The

Table 11
Comparison of TLABC with parameter estimation methods in literature for double diode model.

Item	I_{ph} (A)	I_{sd1} (μA)	R_s (Ω)	R_{sh} (Ω)	a_1	I_{sd2} (μA)	a_2	RMSE
PS	0.7602	0.9889	0.032	81.3008	1.6	0.0001	1.192	1.5180E−02
SA	0.7623	0.4767	0.0345	43.1034	1.5172	1.00E−02	2	1.6640E−02
IGHS	0.7608	0.9731	0.0369	53.8368	1.9213	0.1679	1.4281	9.8635E−04
ABSO	0.76077	0.26713	0.03657	54.6219	1.46512	0.38191	1.98152	9.8344E−04
Rcr-IJADE	0.760781	0.225974	0.03674	55.485443	1.451017	0.749347	2	9.8248E−04
GOFPANM	0.7607811	0.7493476	0.0367404	55.4854485	2	0.2259743	1.4510168	9.8248E−04
IJAYA	0.7601	0.0050445	0.0376	77.8519	1.2186	0.75094	1.6247	9.8293E−04
EHA-NMS	0.760781	0.225974	0.03674	55.485441	1.451017	0.749346	2	9.8248E−04
CWOA	0.76077	0.2415	0.6	1.45651	1.9899	0.03666	55.2016	9.8272E−04
TLABC	0.76081	0.42394	0.03667	54.66797	1.9075	0.24011	1.45671	9.8414E−04

Table 12
Comparison of TLABC with parameter estimation methods in literature for PV module diode model.

Item	I_{ph} (A)	I_{sd} (μA)	R_s (Ω)	R_{sh} (Ω)	a	RMSE
PS	1.03130	3.17560	1.20530	714.28570	48.28890	1.1800E−02
SA	1.03056	3.4715	1.20165	972.93567	48.63131	2.7000E−03
MPCOA	1.0331	3.6642	1.1989	833.3333	48.8211	2.425E−03
Rcr-IJADE	1.03188	3.3737	1.20295	849.6927	48.50646	2.4251E−03
IJAYA	1.0305	3.4703	1.2016	977.3752	48.6298	2.4251E−03
GOFPANM	1.0305143	3.4822631	1.201271	981.9823286	48.6428351	2.425E−03
EHA-NMS	1.030514	3.482263	1.201271	981.98224	48.642835	2.425E−03
TLABC	1.03056	3.4715	1.20165	972.93567	48.63131	2.4251E−03

determined parameters and RMSE values are presented in Table 7. It can be seen that TLABC also obtain the best RMSE (2.42507E−03) among all the algorithms, followed by NIWTLBO, TLBO, LETLBO, GOTLBO, MABC, GBABC, GABC, and ABC. Moreover, the calculated data obtained by TLABC and experimental data are compared in Fig. 6 and Table 8. The *I-V* and *P-V* characteristics of the estimated model are also in quite good agreement with the experimental data, and all the IAE values are smaller than 4.850E−03. The high accuracy parameters are achieved again by the TLABC algorithm.

5.4. Comparison based on statistical results

In this subsection, to compare the average accuracy and reliability of different algorithms, the statistical results including the minimum, mean, maximum, as well as the standard deviation of RMSE for all the compared algorithms over 30 independent runs are presented in Table 9. The mean RMSE quantifies the average accuracy, and the standard deviation (SD) of RMSE indicates the reliability of the parameters estimation methods. For each model, the overall best and the second best results among the nine algorithms are highlighted in gray boldface and boldface, respectively.

For the single diode model, TLABC achieves the best results in terms of minimum RMSE and mean RMSE among the nine algorithms. NIWTLBO achieves the best results in terms of maximum RMSE and standard deviation, and TLABC also exhibits very competitive performance since it achieves the second best results. For the double diode model, TLABC gets the best results in terms of minimum RMSE. NIWTLBO gets the best results in terms of mean RMSE, and ABC gets the best results in terms of standard deviation. For the PV module model, TLABC perform better than all the other algorithms in terms of all statistical indicators, including minimum RMSE, mean RMSE, maximum RMSE and standard deviation.

The convergence curves of TLABC for different PV models are presented in Fig. 7. For the single diode model, TLABC converges to the optimal model parameters at RMSE equal to 9.8602E−04 after 33,851 function evaluations. For the double diode model, TLABC converges to the optimal model parameters at RMSE equal to 9.8414E−04 after 47,321 function evaluations. For the PV module model, TLABC converges to the optimal model parameters at RMSE equal to 2.4251E−03 after 26,851 function evaluations.

Based on these comparisons, it can be concluded that the proposed TLABC has a very competitive performance in terms of solution accuracy and reliability for solving the parameters estimation problems of different PV models.

5.5. Comparison with results in the literature

For the single diode model, the estimated parameters and best RMSE of TLABC are further compared with the results in the literature, including those of GA [16], CPSO [17], PS [49], SA [23], IGHS [24], ABSO [26], Rcr-IJADE [19], IJAYA [39], GOFPANM [2], EHA-NMS [6], and CWOA [4]. These methods are chosen for comparison due to their good performance in the single diode model. The experimental results are presented in Table 10. It can be observed that TLABC, together with GOFPANM, CWOA, EHA-NMS and Rcr-IJADE obtain the best RMSE (9.8602E−04), followed by IJAYA (9.8603E−04), ABSO (9.9124E−04), IGHS (9.9306E−04), CPSO (1.3900E03), PS (1.4940E−02), SA (1.9000E−02), and GA (1.9080E02).

For the double diode model, the estimated parameters and best RMSE value of TLABC are compared with those of PS [49], SA [23], IGHS [24], ABSO [26], Rcr-IJADE [19], IJAYA [39], GOFPANM [2], EHA-NMS [6], and CWOA [4]. Table 11 shows the results of different methods. For this problem, EHA-NMS and Rcr-IJADE achieve the best RMSE (9.82480E−04). TLABC obtain a value of 9.8414E−04, which is better than PS, SA, and IGHS, while worse than other methods.

For PV module model, Table 12 presents the results of PS [49], SA [23], MPCOA [53], Rcr-IJADE [19], IJAYA [39], GOFPANM [2], EHA-NMS [6], and TLABC. From Table 12, it can be seen that TLABC, MPCOA, Rcr-IJADE, IJAYA, GOFPANM, and EHA-NMS obtain the best RMSE (2.425E−03), followed by SA (2.7000E−03) and PS (1.1800E−02).

Based on the aforementioned comparisons, it demonstrates that TLABC can achieve similar or better results compared with these methods in the literature; therefore, it can be used an efficient and reliable alternative method for parameter identification problems in different PV models.

6. Conclusion

In this paper, a new hybrid teaching-learning-based artificial bee colony (TLABC) algorithm has been proposed for effectively and accurately estimating the parameters of different PV models, by

combining the features of teaching-learning-based optimization (TLBO) with artificial bee colony (ABC). In the proposed method, three hybrid search phases, namely teaching-based employed bee phase, learning-based on looker bee phase, and generalized oppositional scout bee phase are employed to enhance the search abilities. TLABC is applied to solve the parameters estimation problems of single diode, double diode, and PV module models. The results of TLABC are compared with well-established TLBO and ABC algorithms, as well as those results reported in the literature. Experimental results show that TLABC has a very competitive performance in terms of accuracy and reliability. Therefore, TLABC can serve as a new alternative method for parameter estimation problems of solar photovoltaic models.

Acknowledgements

This work was supported in part by the Natural Science Foundation of Jiangsu Province (Grant No. BK 20160540), the China Postdoctoral Science Foundation (Grant No. 2016M591783), the National Natural Science Foundation of China (Grant No. 61703268), the Research Talents Startup Foundation of Jiangsu University (Grant No. 15JDG139), the Fundamental Research Funds for the Central Universities (Grant No. 222201717006), and the PAPD of Jiangsu Higher Education Institutions.

References

[1] Muhsen DH, Ghazali AB, Khatib T, Abed IA. Parameters extraction of double diode photovoltaic module's model based on hybrid evolutionary algorithm. Energy Convers Manage 2015;105:552–61.
[2] Xu S, Wang Y. Parameter estimation of photovoltaic modules using a hybrid flower pollination algorithm. Energy Convers Manage 2017;144:53–68.
[3] [REN21]–Renewable Energy Policy Network for the 21st Century, 2017. Renewables 2017—global status report. Paris: REN21; 2017. http://www.ren21.net/gsr-2017.
[4] Oliva D, El Aziz MA, Hassanien AE. Parameter estimation of photovoltaic cells using an improved chaotic whale optimization algorithm. Appl Energy 2017;200:141–54.
[5] Singh GK. Solar power generation by PV (photovoltaic) technology: a review. Energy 2013;53:1–13.
[6] Chen Z, Wu L, Lin P, Wu Y, Cheng S. Parameters identification of photovoltaic models using hybrid adaptive Nelder-Mead simplex algorithm based on eagle strategy. Appl Energy 2016;182:47–57.
[7] Yu K, Chen X, Wang X, Wang Z. Parameters identification of photovoltaic models using self-adaptive teaching-learning-based optimization. Energy Convers Manage 2017;145:233–46.
[8] Ma J, Bi Z, Ting TO, Hao S, Hao W. Comparative performance on photovoltaic model parameter identification via bio-inspired algorithms. Sol Energy 2016;132:606–16.
[9] Guo L, Meng Z, Sun Y, Wang L. Parameter identification and sensitivity analysis of solar cell models with cat swarm optimization algorithm. Energy Convers Manage 2016;108:520–8.
[10] Easwarakhanthan T, Bottin J, Bouhouch I, Boutrit C. Nonlinear minimization algorithm for determining the solar cell parameters with microcomputers. Int J Sol Energy 1986;4:1–12.
[11] Ortiz-Conde A, Sánchez FJG, Muci J. New method to extract the model parameters of solar cells from the explicit analytic solutions of their illuminated I-V characteristics. Sol Energy Mater Sol Cells 2006;90:352–61.
[12] Chan D, Phillips J, Phang J. A comparative study of extraction methods for solar cell model parameters. Solid-State Electron 1986;29:329–37.
[13] Chen X, Yu K, Du W, Zhao W, Liu G. Parameters identification of solar cell models using generalized oppositional teaching learning based optimization. Energy 2016;99:170–80.
[14] Jervase JA, Bourdoucen H, Al-Lawati A. Solar cell parameter extraction using genetic algorithms. Meas Sci Technol 2001;12:1922.
[15] Zagrouba M, Sellami A, Bouaïcha M, Ksouri M. Identification of PV solar cells and modules parameters using the genetic algorithms: application to maximum power extraction. Solar Energy 2010;84:860–6.
[16] AlRashidi M, AlHajri M, El-Naggar K, Al-Othman A. A new estimation approach for determining the I-V characteristics of solar cells. Sol Energy 2011;85:1543–50.
[17] Wei H, Cong J, Lingyun X, Deyun S. Extracting solar cell model parameters based on chaos particle swarm algorithm. In: International conference on electric information and control engineering (ICEICE), IEEE; 2011. p. 398–402.
[18] Jordehi AR. Time varying acceleration coefficients particle swarm optimisation (TVACPSO): a new optimisation algorithm for estimating parameters of PV cells and modules. Energy Convers Manage 2016;129:262–74.
[19] Gong W, Cai Z. Parameter extraction of solar cell models using repaired adaptive differential evolution. Sol Energy 2013;94:209–20.
[20] Ishaque K, Salam Z, Mekhilef S, Shamsudin A. Parameter extraction of solar photovoltaic modules using penalty-based differential evolution. Appl Energy 2012;99:297–308.
[21] Ayala HVH, dos Santos Coelho L, Mariani VC, Askarzadeh A. An improved free search differential evolution algorithm: a case study on parameters identification of one diode equivalent circuit of a solar cell module. Energy 2015;93:1515–22.
[22] Chellaswamy C, Ramesh R. Parameter extraction of solar cell models based on adaptive differential evolution algorithm. Renew Energy 2016;97:823–37.
[23] El-Naggar K, AlRashidi M, AlHajri M, Al-Othman A. Simulated annealing algorithm for photovoltaic parameters identification. Sol Energy 2012;86:266–74.
[24] Askarzadeh A, Rezazadeh A. Parameter identification for solar cell models using harmony search-based algorithms. Sol Energy 2012;86:3241–9.
[25] Niu Q, Zhang H, Li K. An improved TLBO with elite strategy for parameters identification of PEM fuel cell and solar cell models. Int J Hydrogen Energy 2014;39:3837–54.
[26] Askarzadeh A, Rezazadeh A. Artificial bee swarm optimization algorithm for parameters identification of solar cell models. Appl Energy 2013;102:943–9.
[27] Oliva D, Cuevas E, Pajares G. Parameter identification of solar cells using artificial bee colony optimization. Energy 2014;72:93–102.
[28] Niu Q, Zhang L, Li K. A biogeography-based optimization algorithm with mutation strategies for model parameter estimation of solar and fuel cells. Energy Convers Manage 2014;86:1173–85.
[29] Hasanien HM. Shuffled frog leaping algorithm for photovoltaic model identification. IEEE Trans Sustain Energy 2015;6:509–15.
[30] Ma J, Ting T, Man KL, Zhang N, Guan S-U, Wong PW. Parameter estimation of photovoltaic models via cuckoo search. J Appl Math 2013;2013.
[31] Alam D, Yousri D, Eteiba M. Flower pollination algorithm based solar PV parameter estimation. Energy Convers Manage 2015;101:410–22.
[32] Ram JP, Babu TS, Dragicevic T, Rajasekar N. A new hybrid bee pollinator flower pollination algorithm for solar PV parameter estimation. Energy Convers Manage 2017;135:463–76.
[33] Awadallah MA. Variations of the bacterial foraging algorithm for the extraction of PV module parameters from nameplate data. Energy Convers Manage 2016;113:312–20.
[34] Allam D, Yousri D, Eteiba M. Parameters extraction of the three diode model for the multi-crystalline solar cell/module using Moth-Flame Optimization Algorithm. Energy Convers Manage 2016;123:535–48.
[35] Fathy A, Rezk H. Parameter estimation of photovoltaic system using imperialist competitive algorithm. Renew Energy 2017;111:307–20.
[36] Kler D, Sharma P, Banerjee A, Rana K, Kumar V. PV cell and module efficient parameters estimation using Evaporation Rate based Water Cycle Algorithm. Swarm Evol Comput 2017.
[37] Wu Z, Yu D, Kang X. Parameter identification of photovoltaic cell model based on improved ant lion optimizer. Energy Convers Manage 2017;151:107–15.
[38] Ali E, El-Hameed M, El-Fergany A, El-Arini M. Parameter extraction of photovoltaic generating units using multi-verse optimizer. Sustain Energy Technol Assess 2016;17:68–76.
[39] Yu K, Liang J, Qu B, Chen X, Wang H. Parameters identification of photovoltaic models using an improved JAYA optimization algorithm. Energy Convers Manage 2017;150:742–53.
[40] Wang L, Huang C. A novel Elite Opposition-based Jaya algorithm for parameter estimation of photovoltaic cell models. Optik-Int J Light Electron Opt 2018;155:351–6.
[41] Das S, Suganthan PN. Differential evolution: a survey of the state-of-the-art. IEEE Trans Evol Comput 2011;15:4–31.
[42] Rao R, Savsani V, Vakharia D. Teaching–learning-based optimization: an optimization method for continuous non-linear large scale problems. Inf Sci 2012;183:1–15.
[43] Karaboga D, Basturk B. A powerful and efficient algorithm for numerical function optimization: artificial bee colony (ABC) algorithm. J Global Optim 2007;39:459–71.
[44] Zou F, Wang L, Hei X, Chen D, Yang D. Teaching–learning-based optimization with dynamic group strategy for global optimization. Inf Sci 2014;273:112–31.
[45] Zhu G, Kwong S. Gbest-guided artificial bee colony algorithm for numerical function optimization. Appl Math Comput 2010;217:3166–73.
[46] Price K, Storn RM, Lampinen JA. Differential evolution: a practical approach to global optimization. Springer Science & Business Media; 2006.
[47] Zhou X, Wu Z, Wang H, Rahnamayan S. Gaussian bare-bones artificial bee colony algorithm. Soft Comput 2014:1–18.
[48] Wang H, Wu Z, Rahnamayan S, Liu Y, Ventresca M. Enhancing particle swarm optimization using generalized opposition-based learning. Inf Sci 2011;181:4699–714.
[49] AlHajri M, El-Naggar K, AlRashidi M, Al-Othman A. Optimal extraction of solar cell parameters using pattern search. Renew Energy 2012;44:238–45.
[50] Wu Z-S, Fu W-P, Xue R. Nonlinear inertia weighted teaching-learning-based optimization for solving global optimization problem. Comput Intell Neurosci 2015;2015:87.
[51] Zou F, Wang L, Hei X, Chen D. Teaching–learning-based optimization with learning experience of other learners and its application. Appl Soft Comput 2015;37:725–36.
[52] Akay B, Karaboga D. A modified artificial bee colony algorithm for real-parameter optimization. Inf Sci 2012;192:120–42.
[53] Yuan X, Xiang Y, He Y. Parameter extraction of solar cell models using mutative-scale parallel chaos optimization algorithm. Sol Energy 2014;108:238–51.